Jadarite, LiNaSiB$_3$O$_7$(OH), a new mineral species from the Jadar Basin, Serbia

Christopher J. Stanley[1],[*], Gary C. Jones[1], Michael S. Rumsey[1], Christopher Blake[2], Andrew C. Roberts[3], John A.R. Stirling[3], Graham J.C. Carpenter[4], Pamela S. Whitfield[5], Joel D. Grice[6] and Yvon LePage[5]

[1] Department of Mineralogy, Natural History Museum, London SW7 5BD, UK
*Corresponding author, e-mail: c.stanley@nhm.ac.uk
[2] Rio Tinto, Unit 34 Hither Green Ind. Est., Clevedon, North Somerset, BS21 6XU, UK
[3] Geological Survey of Canada, 601 Booth Street, Ottawa, Ontario, K1A 0E8, Canada
[4] Materials Technology Laboratories, Natural Resources Canada, 568 Booth Street, Ottawa, Ontario, K1A 0G1, Canada
[5] Institute for Chemical Process and Environmental Technology, National Research Council Canada,
1200 Montreal Road, Ottawa, Ontario, K1A 0R6, Canada
[6] Canadian Museum of Nature, P.O. Box 3443, Station "D", Ottawa, Ontario, K1P 6P4, Canada

Abstract: Jadarite, ideally LiNaSiB$_3$O$_7$(OH), is a new mineral species from the Jadar Basin, Serbia. It occurs as massive white aggregates, several metres thick, and is relatively free from inclusions and intergrowths; however, individual subhedral (tabular, elongate) to anhedral crystals rarely exceed 5−10 μm in size. It is associated with calcite, dolomite, K-feldspar, rutile, albite, ilmenite, pyrite, and fine-grained muscovite. Searlesite, analcime, chlorite, and quartz have also been identified. Jadarite is translucent (opaque in masses) with a porcellanous lustre (masses), possesses a white streak, is brittle with a platy habit and has an uneven to conchoidal fracture. VHN$_{200}$ is 390 (range 343−426) kg/mm^2. Mohs' hardness is 4−5. It shows weak pink-orange fluorescence under both short- and long-wave ultraviolet radiation. An infra-red adsorption spectrum is given and shows strong, sharp peaks at 3490 and 3418 cm^{-1} which indicates that water is present as (OH) only. Peaks at 1409 and 1335 cm^{-1} indicate the presence of BO$_3$ groups, and between 900 and 1180 cm^{-1} the probable presence of BO$_4$. In transmitted light, plates and grains of jadarite show twinning in some crystallites and for λ 590 nm n_α = 1.536(±0.001) and n_γ = 1.563(±0.001). It is non-pleochroic, biaxial, and does not show parallel extinction. In plane-polarized reflected light, the mineral is dark grey with weak bireflectance, it is non-pleochroic and has abundant white internal reflections. Wet chemical analysis combined with CHN analyzer gave the following aggregate composition: Li$_2$O 7.3, Na$_2$O 15.0, SiO$_2$ 26.4, B$_2$O$_3$ 47.2, H$_2$O 4.3, total 100.2 wt.%. The empirical formula, based on 3 B atoms per formula unit (*apfu*), is: Li$_{1.08}$Na$_{1.07}$Si$_{0.97}$B$_3$O$_{6.99}$(OH)$_{1.06}$. Jadarite is monoclinic (*P*2$_1$/*n*) with *a* 6.818(2), *b* 13.794(2), *c* 6.756(2) Å, β 111.10(2)° *V* 592.8(2) Å^3 (*Z* = 4), alternatively (*P*2$_1$/*c*) with *a* 6.756(3), *b* 13.794(2), *c* 7.680(3) Å, β 124.07(3)°, *V* 592.9(4) Å^3 and *Z* = 4. The measured density (Berman Balance) is 2.45 g/cm^3; calculated density is 2.46 g/cm^3 (on the basis of the empirical formula and unit-cell parameters refined from powder data). The six strongest X-ray powder-diffraction lines [$\overline{d}$ in Å(*I*)(*hkl*)] are: 4.666 (62) (120, 021), 3.180 (82) (200), 3.152 (74) (002), 3.027 (40) (2 21), 2.946 (100) (131), 2.241 (74) (3 11,151), The mineral name is for the locality in Serbia where it was discovered during mineral exploration of the Jadar Basin.

Key-words: jadarite, new mineral species, lithium sodium borosilicate hydroxide, Jadar Basin, Serbia, chemical data, infra-red absorption spectrum, X-ray powder-diffraction data.

Introduction

Jadarite is a new lithium sodium borosilicate mineral which was discovered in drill core from a borehole in the Jadar Basin, Serbia (44º32′ N, 19º18′ Jadap The name is after the locality; in Serbian Cyrillic: , in Russian Cyrillic: , hence the pronunciation is YĂDĂRITE. The mineral and mineral name were approved by the Commision on New Minerals, Nomenclature and Classifica-

tion (CNMNC), International Mineralogical Association (2006−36). Holotype material is deposited at the Natural History Museum, London, UK as BM 2006, 16. Parts of the holotype are housed within the Systematic Reference Series of the National Mineral Collection of Canada, Geological Survey of Canada, Ottawa under catalogue number NMCC 068101, and cotype fragments have also been donated to the Natural History Museum, Budapest, Hungary and to the Belgrade Natural History Museum, Belgrade, Serbia.
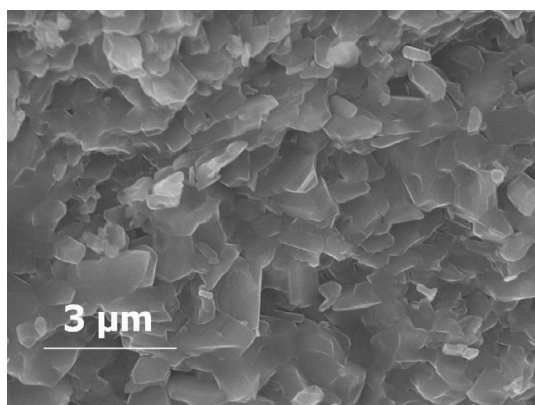
Fig. 1. A secondary-electron image illustrating the nature of jadarite (various grey shades).The new mineral exhibits a relatively tabular nature and discrete crystallites rarely exceed 5 μm in size. Note the presence of small cavities between the crystallites that give it a pitted appearance when examined in polished section. Width of view is 12 μm.
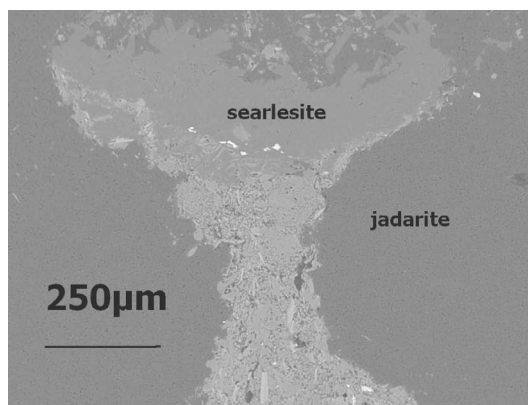

Fig. 2. A backscattered-electron image illustrating the presence of searlesite (medium grey) that is closely associated with jadarite (dark grey) and fine-grained matrix (light grey). Note the porous/pitted nature of jadarite. Width of view is 1 mm.

Occurrence

The Jadar Basin is composed of a sequence of oil-shales, dolomicrites and pyroclastic deposits of Neogene (Early to Middle Miocene) age, and includes evaporites which formed during the development of the intramontane lacustrine sedimentary basin (Obradovic *et al.*, 1997). Jadarite occurs as massive white aggregates (several metres thick in drill core) that are relatively free from inclusions and intergrowths. It also occurs as millimetre-sized nodular aggregates within the fine-grained carbonate and mica-rich matrix. Detailed examination of the fine-grained matrix associated with jadarite revealed the presence of calcite, dolomite, K-feldspar, rutile, albite, ilmenite, pyrite, and fine-grained muscovite. Minor amounts of searlesite [ideally $NaBSi_2O_5(OH)_2$] are also often intergrown with jadarite. Analcime [ideally $NaAlSi_2O_6.(H_2O)$], chlorite, and quartz have also been identified.

Physical properties

Jadarite occurs as minute (5−10 μm) subhedral (tabular, elongate) to anhedral grains (Fig. 1). Aggregates of jadarite in hand specimen have a porcellanous lustre and give a white streak. Jadarite is brittle with an uneven to conchoidal fracture and a platy habit. Aggregates of crystallites exhibit a degree of porosity (Fig. 2). Indentation hardness measurements gave $VHN_{200} = 390$ (range 343−426) kg/mm^2, which is in good agreement with the Mohs' hardness of 4−5 determined on the basis that jadarite aggregates scratch fluorite and are scratched by apatite. The density was obtained using a Berman Balance and an average of ten measurements gave a measured density of 2.45 g/cm^3 which is in good agreement with the calculated density of 2.46 g/cm^3 obtained from the empirical formula and unit-cell parameters refined from powder data. Jadarite shows weak pink-orange fluorescence under both short- and long-wave ultraviolet radiation.

Optical properties

Jadarite was crushed and then microscopically examined in transmitted light before determination of refractive indices with refractive index liquids. The plates and grains of about 5 μm showed twinning in some crystallites with extinction at 8° either side of the twin plane. Jadarite is non-pleochroic and does not show parallel extinction. It is biaxial, in agreement with its monoclinic symmetry, and has for λ 590 nm $n_\alpha = 1.536(\pm0.001)$ and $n_\gamma = 1.563(\pm0.001)$.

The sample containing jadarite was prepared for reflected light optical investigation and reflectance measurement using standard diamond polishing techniques (*e.g.* Stanley & Laflamme, 1998). In order to minimize any internal reflections which might affect the quantitative reflectance measurements, the jadarite specimen was cut and then mounted in the form of a wedge with sharp angle about 20°. In plane-polarized reflected light (from an unfiltered quartz-halogen lamp at about 3100 K), jadarite is dark-grey in colour, with weak bireflectance, no observable pleochroism, and any possible anisotropy masked by abundant white internal reflections.

Reflectance measurements were made with a Zeiss microspectrophotometer relative to a cubic zirconia reflectance standard, using the equipment and procedures reported by Criddle in Berlepsch *et al.*, (2003). Measurements were made over an area of about 400 μm^2 and are thus an average of many grains in different orientations. At $\lambda = 589$ nm, the refractive index, calculated from the Fresnel equation (assuming k is 0), is 1.54, which is in reasonable agreement with the results in transmitted light given above.

Infra-red spectroscopy

The infra-red absorption spectrum is given in Fig. 3. The sample was run "as received" (not dried in order to avoid possible dehydration) in a KBr disk using a Perkin Elmer Spectrum One FTIR instrument. The complexity
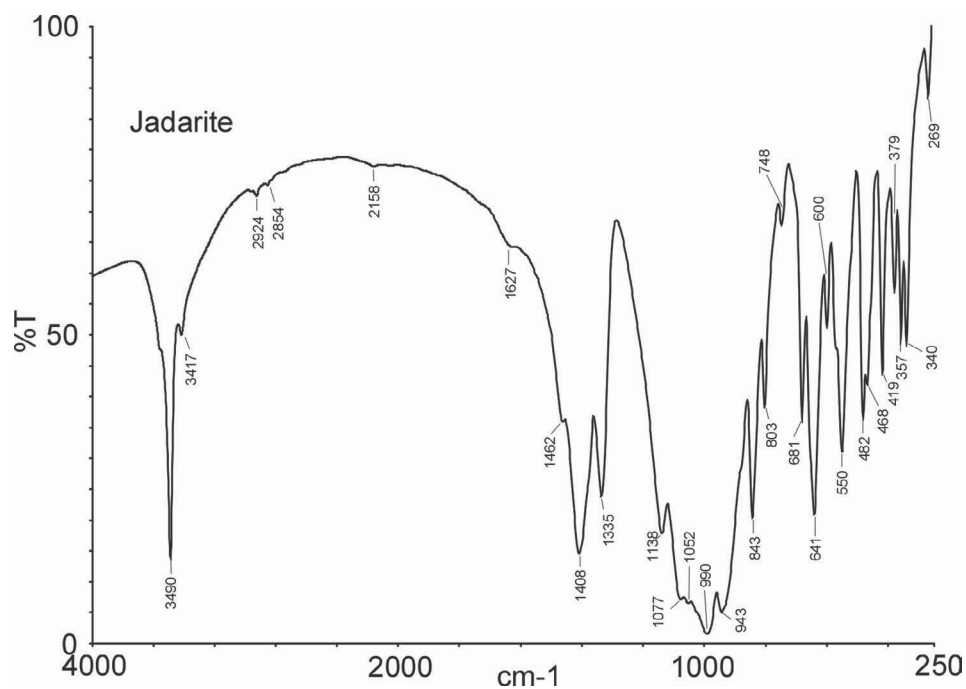
Fig. 3. Infra-red absorption spectrum for jadarite.

and sharpness of the spectrum is typical of borosilicates. The strong, sharp peaks at 3490 and 3418 cm^{-1} indicate that water is present as (OH) only. Peaks at 1409 and 1335 cm^{-1} indicate the presence of BO$_3$ groups, *i.e.*, trigonal boron (given the absence of carbonate). Absorptions in the 900–1180 cm^{-1} region may indicate the presence of BO$_4$ groups, *i.e.*, tetrahedral boron, but the complexity of the spectrum below 1200 cm^{-1} makes peak assignment difficult. The "tentative" peak assignments in Table 1 were suggested by an anonymous reviewer of the CNMNC submission.

Chemical composition

Material for analysis was dried at 110 °C for one hour. Wet chemical analyses were performed on solutions from lithium metaborate fusions for Na, Si and other cations, plus sodium carbonate fusions for Li and B. The analyses were carried out by inductively coupled plasma atomic emission spectrophotometry (ICPAES) using a Varian VistaPro (axial) instrument combined with a CHNS (combustion) analyzer (Thermo Finnigan Flash EA112) for carbon and water, and gave the following aggregate composition: Li$_2$O 7.3, Na$_2$O 15.0, SiO$_2$ 26.4, B$_2$O$_3$ 47.2, H$_2$O 4.3, total 100.2 wt.%. The empirical formula based on 3 B atoms per formula unit (*apfu*), is: Li$_{1.08}$Na$_{1.07}$Si$_{0.97}$B$_3$O$_{6.99}$(OH)$_{1.06}$. The simplified formula is LiNaSiB$_3$O$_7$(OH) which requires: Li$_2$O 6.81, Na$_2$O 14.12, SiO$_2$ 27.38, B$_2$O$_3$ 47.59, H$_2$O 4.11, total 100.01 wt.%. Jadarite is easily soluble in cold dilute (approx 0.5 M) mineral acids, *e.g.*, HCl, HNO$_3$ and H$_2$SO$_4$. It appears to be insoluble in water.

Table 1. Infra-red absorption data for jadarite.

Wavenumbers (cm^{-1})	Tentative assignment
3480	OH (literature suggests B(OH)$_4$), valence
3418	" " " " " "
1409	trigonal borate group, valence
1335	B-OH, deformation or trigonal borate, valance
1138	
990	SiO$_4$/BO$_4$, valance
943	
843	B-OH, deformation?
803	tetrahedral borate group, valence
748	" " " "
681	B(OH)$_4$, deformation?
641	
600	
551	
482	
469	trigonal and tetrahedral borate, deformation
420	" " " " "
379	
358	" " " " "
340	" " " " "
270	" " " " "

X-ray diffraction and TEM studies

X-ray powder diffraction

A CoKα Bruker D8 Advance powder diffractometer was used to obtain the fully-indexed X-ray powder data presented in Table 2. This was indexed on a primitive monoclinic unit cell of *a* 6.818(2), *b* 13.794(2),

Table 2. X-ray powder-diffraction data for jadarite.

I_{est}	$d\text{Å}_{(meas.)}$	$d\text{Å}_{(calc.)}$	hkl	hkl[1]	I_{est}	$d\text{Å}_{(meas.)}$	$d\text{Å}_{(calc.)}$	hkl	hkl[1]
* 34	6.889	6.897	020	020	7	1.912	1.911	033	$\bar{3}$33
6	5.731	5.733	011	$\bar{1}$11	16	1.896	1.897	$\bar{3}$41	142
* 14	5.592	5.597	$\bar{1}$01	100			1.894	$\bar{1}$62	$\bar{2}$61
5	5.182	5.186	$\bar{1}$11	110	9	1.884	1.885	$\bar{1}$43	$\bar{3}$42
		4.676	120	021	* 20	1.850	1.849	222	$\bar{2}$24
62	4.666	4.653	021	$\bar{1}$21	* 13	1.827	1.827	$\bar{3}$42	241
* 30	4.343	4.346	$\bar{1}$21	120	3	1.807	1.806	340	043
2	3.840	3.839	101	$\bar{1}$02	2	1.775	1.776	$\bar{2}$62	260
* 39	3.716	3.715	031	$\bar{1}$31	8	1.753	1.753	171	$\bar{1}$72
* 30	3.447	3.449	040	040	1	1.724	1.724	080	080
* 21	3.355	3.355	121	$\bar{1}$22	* 12	1.694	1.693	331	$\bar{1}$34
* 82	3.180	3.180	200	002	* 15	1.683	1.685	133	$\bar{3}$34
* 74	3.152	3.152	002	$\bar{2}$02	* 10	1.664	1.663	081	$\bar{1}$81
9	3.099	3.099	210	012	* 18	1.647	1.648	$\bar{1}$81	180
* 24	3.073	3.072	012	$\bar{2}$12	4	1.630	1.629	$\bar{1}$24	$\bar{4}$23
* 40	3.027	3.027	$\bar{2}$21	121	3	1.609	1.608	$\bar{1}$63	$\bar{3}$62
* 28	3.009	3.008	$\bar{1}$22	$\bar{2}$21	* 16	1.573	1.573	181	$\bar{1}$82
* 100	2.946	2.947	131	$\bar{1}$32			1.548	271	$\bar{1}$73
* 10	2.867	2.866	022	$\bar{2}$22	4	1.546	1.545	$\bar{3}$53,172	350, $\bar{2}$73
8	2.798	2.798	$\bar{2}$02	200			1.536	024	$\bar{4}$24
4	2.704	2.704	$\bar{1}$32	$\bar{2}$31	2	1.535	1.535	$\bar{2}$81	181
4	2.600	2.600	032	$\bar{2}$32			1.532	$\bar{1}$82	$\bar{2}$81
4	2.530	2.531	150	051	6	1.520	1.520	351	$\bar{1}$54
4	2.461	2.460	211	$\bar{1}$13			1.516	280	082
4	2.390	2.390	$\bar{2}$32	230	14	1.514	1.514	$\bar{4}$42	242
* 12	2.338	2.338	240	042			1.513	082	$\bar{2}$82
4	2.298	2.299	060	060	3	1.504	1.503	430	034
* 36	2.272	2.272	$\bar{3}$01	102			1.491	034	$\bar{4}$34
* 38	2.252	2.251	$\bar{1}$03	$\bar{3}$02	8	1.490	1.489	091	$\bar{1}$91
		2.242	$\bar{3}$11	112	5	1.468	1.468	$\bar{2}$82	280
74	2.241	2.240	151	$\bar{1}$52	7	1.445	1.444	440	044
2	2.191	2.189	132	$\bar{2}$33	5	1.423	1.422	163	$\bar{3}$64
		2.162	160	061	3	1.421	1.420	281	$\bar{1}$83
32	2.160	2.160	061	$\bar{1}$61	4	1.400	1.399	$\bar{4}$04	400
* 12	2.134	2.134	$\bar{2}$51	151	6	1.393	1.392	$\bar{4}$14	410
9	2.078	2.076	052	$\bar{3}$13			1.378	450	054
* 15	2.047	2.047	$\bar{2}$23	$\bar{3}$21	10	1.376	1.375	272	$\bar{2}$74
		2.024	241	$\bar{1}$43	3	1.356	1.355	$\bar{1}$64,$\bar{3}$73	$\bar{4}$63,370
12	2.022	2.019	142	$\bar{2}$43	4	1.345	1.344	$\bar{5}$01	104
* 11	1.972	1.972	161	$\bar{1}$62	7	1.339	1.339	$\bar{1}$101,$\bar{4}$34	1100,430
7	1.951	1.951	$\bar{3}$32	231	2	1.326	1.325	$\bar{1}$15	$\bar{5}$14
* 11	1.943	1.943	$\bar{2}$33	$\bar{3}$31					
		1.925	330	033					
4	1.923	1.920	202	$\bar{2}$04					

Bruker D8 Advance powder diffractometer using Co radiation (λ Co$K\alpha_1$ = 1.78892 Å). External Si standard with variable divergence and antiscattering slits. Sample run from 2 to 86°2θ with a step size of 0.01° and a time per step of 5 s. *: Lines used for unit-cell refinement. Indexed on *a* 6.818(2), *b* 13.794(2), *c* 6.756(2) Å, β 111.10(2)° (for space group $P2_1/n$). [1] = $P2_1/c$ monoclinic indexing of Whitfield *et al.* (2007); indexed on *a* 6.756(3), *b* 13.794(2), *c* 7.680(3) Å, β 124.07(3)°.

c 6.756(2) Å, *β* 111.10(2)° and possible space group *P*2₁/*n*. The cell volume is 592.8(2) Å³ and *Z* = 4.

Jadarite "crystals" are much too small to even attempt single-crystal studies by classical methods. Hence, the X-ray powder-diffraction data collected on the Bruker diffractometer was run through a series of auto-indexing programs which collectively constitute the CRYSFIRE suite (Shirley, 2002). A possible primitive monoclinic cell with a high Figure of Merit (FOM) was encountered using Dicvol91 (Boultif & Louër, 1991); this potential cell indexed all the observed reflections and, in addition, had a unit-cell volume (592 Å³) appreciably lower than any of the other potential candidates. Subsequently, pure jadarite material was selected for TEM electron-diffraction studies using selected-area (SAED) and convergent-beam (CBED) techniques by one of us (GJCC) Three different zones were examined and a primitive unit-cell volume of approximately 576 Å³ was determined from various convergent beam patterns on two different zones using the method of LePage & Downham (1991). This CBED-determined cell volume is consistent with that calculated by the Dicvol91 auto-indexing program and strongly supports our assignment of the primitive monoclinic cell.

Additional pure material was given to one of us (PSW) who has successfully determined the structure of jadarite by indexing, simulated annealing and Rietveld refinement of data from a separate capillary sample on a Cu*Kα* Bruker D8 diffractometer. The jadarite structure was refined in monoclinic *P*2₁/*c* with *a* 6.7620(1), *b* 13.8016(3), *c* 7.6878(2) Å, *β* 124.0894(9)° (Whitfield *et al.*, 2007)), which is the Parthé convention setting of the *P*2₁/*n* cell. Details of the structure have been published elsewhere and are illustrated in Fig. 4. The structure contains a layer of corner-sharing, tetrahedrally coordinated Li, Si, B which form an unbranched *vierer* single layer that is, in turn, decorated with triangular BO₃ groups. The Na atom is situated between the tetrahedral layers in a distorted octahedral site. Re-indexing of the powder data in Table 2 has led to the following refined unit-cell parameters for space group *P*2₁/*c* : *a* 6.756(3), *b* 13.794(2), *c* 7.680(3) Å, *β* 124.07(3)°, *V* 592.9(4) Å³ with *Z* = 4. The use of the Parthé cell with the *c* glide plane as opposed to the cell metric with the *n* glide plane simplified the description of the jadarite crystal structure. The *P*2₁/*c* is changed to the *P*2₁/*n* setting by applying the matrix transformation (101, 010, $\bar{1}$00) to the *P*2₁/*c* cell.

Transmission Electron Microscopy

Specimens were prepared by grinding a small piece of the mineral to form a fine powder, which was then supported on a holey carbon film. Individual crystallites were selected to be tilted onto a prominent zone axis and diffraction patterns were recorded using both selected-area diffraction and convergent beam micro-diffraction. A polycrystalline gold specimen was used to calibrate the microscope in diffraction mode. This should result in d-spacing errors to be no worse than 1 ~ 2 %. The errors in angles are estimated to be good to +/ − 1 degree.
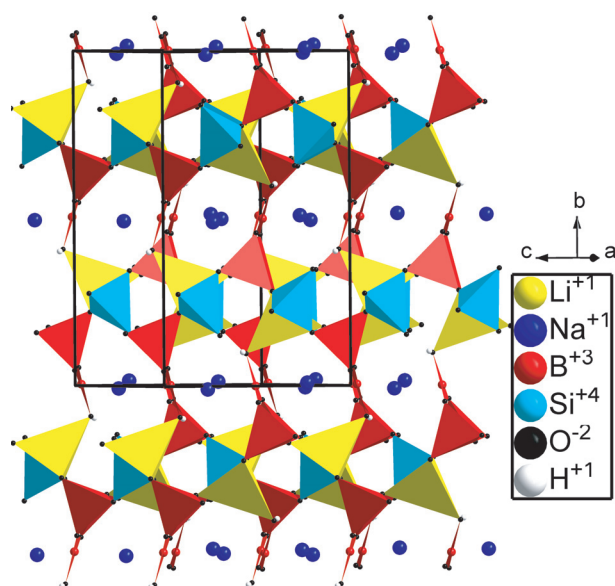

Fig. 4. View of the *P*2₁/*c* jadarite structure along the 010 plane, showing the borosilicate layers bound together with the triangular coordinated BO₃ and octahedral NaO₆. Although not easily visible, the hydrogen is bound to one of the oxygen atoms at the apex of the BO₃ groups.

The mineral was fairly resistant to the 200 kV electron beam, as long as a high beam intensity was not used. Above a critical beam intensity, typically with the beam focused to a fine spot, the mineral quickly became amorphous and hole drilling occurred.

Discussion

Sodium-lithium borosilicate-glass frits are used in nuclear-industry vitrification processes for high-level waste (Roderick *et al.,* 2000). The relationship of jadarite to these (if any) is not clear at present. However, jadarite may well be one of the decomposition products of such glass frits on devitrification and hydration.

References

Berlepsch, P., Armbruster, T., Brugger, J., Criddle, A.J., Graeser, S. (2003): Tripuhyite, FeSbO₄, revisited. *Min. Mag.*, **67**, 31-46.

Boultif, A. & Louër, D. (1991): Indexing of powder diffraction patterns for low-symmetry lattices by the successive dichotomy method. *J. Appl. Crysta.*, **24**, 987-993.

LePage, Y. & Downham, D.A. (1991): Primitive unit cell volumes obtained from unindexed convergent-beam electron diffraction patterns, *J. Electron Microscopy Technology*, **18**, 437-439.

Obradovic, J., Djurdjevic-Colson, J., Vasic, N. (1997): Phytogenic lacustrine sedimentation – oil shales in Neogene from Serbia, Yugoslavia. *J. Palaeolimnology*, **18**, 351-364.

Roderick, J.M., Holland, D., Scales, C.R. (2000): Characterisation and radiation resistance of a mixed alkali borosilicate glass for high level waste vitrification. *Phys. Chem. Glass*, **41**, 392-395.

Shirley, R. (2002): The CRYSFIRE System for Automatic Powder Indexing: User's Manual, The Lattice Press, 41 Guildford Park Avenue, Guildford, Surrey GU2 7NL, England, UK.

Stanley, C.J. & Laflamme, J.H.G. (1998): Preparation of specimens for advanced ore-mineral and environmental studies. Chapter 3. *in* "Modern Approaches to Ore and Environmental Mineralogy" Cabri, L.J. & Vaughan, D.J. (eds.) *Mineral. Ass. Can. Short Course Series*, **27,** 111-121.

Whitfield, P.S., LePage, Y., Grice, J.D., Stanley, C.J., Jones, G.C., Rumsey, M.S., Blake, C., Roberts, A.C., Stirling, J.A.R., Carpenter G.J.C. (2007): $LiNaSiB_3O_7(OH)$ - novel structure of the new borosilicate mineral jadarite, determined from laboratory powder diffraction data. *Acta Cryst. B.*, **B63**, 396-401.